The Astrophysical Journal, 795:46 (8pp), 2014 November 1 doi:10.1088/0004-637X/795/1/46

PREDICTION OF SOLAR ACTIVITY FROM SOLAR BACKGROUND MAGNETIC FIELD VARIATIONS IN CYCLES 21–23

Simon J. Shepherd[1], Sergei I. Zharkov[2], and Valentina V. Zharkova[3]
[1] School of Engineering, University of Bradford, Bradford, BD7 1DP, UK; s.j.shepherd@brad.ac.uk
[2] Department of Physics and Mathematics, University of Hull, Kingston upon Tyne, HU6 7RS, UK; s.zharkov@hull.ac.uk
[3] Department of Mathematics and Information Systems, University of Northumbria, Newcastle upon Tyne, NE2 8ST, UK; valentina.zharkova@northumbria.ac.uk
Received 2014 June 9; accepted 2014 August 25; published 2014 October 13

ABSTRACT

A comprehensive spectral analysis of both the solar background magnetic field (SBMF) in cycles 21–23 and the sunspot magnetic field in cycle 23 reported in our recent paper showed the presence of two principal components (PCs) of SBMF having opposite polarity, e.g., originating in the northern and southern hemispheres, respectively. Over a duration of one solar cycle, both waves are found to travel with an increasing phase shift toward the northern hemisphere in odd cycles 21 and 23 and to the southern hemisphere in even cycle 22. These waves were linked to solar dynamo waves assumed to form in different layers of the solar interior. In this paper, for the first time, the PCs of SBMF in cycles 21–23 are analyzed with the symbolic regression technique using Hamiltonian principles, allowing us to uncover the underlying mathematical laws governing these complex waves in the SBMF presented by PCs and to extrapolate these PCs to cycles 24–26. The PCs predicted for cycle 24 very closely fit (with an accuracy better than 98%) the PCs derived from the SBMF observations in this cycle. This approach also predicts a strong reduction of the SBMF in cycles 25 and 26 and, thus, a reduction of the resulting solar activity. This decrease is accompanied by an increasing phase shift between the two predicted PCs (magnetic waves) in cycle 25 leading to their full separation into the opposite hemispheres in cycle 26. The variations of the modulus summary of the two PCs in SBMF reveals a remarkable resemblance to the average number of sunspots in cycles 21–24 and to predictions of reduced sunspot numbers compared to cycle 24: 80% in cycle 25 and 40% in cycle 26.

Key words: dynamo – methods: data analysis – Sun: activity – Sun: magnetic fields – sunspots

Online-only material: color figures

1. INTRODUCTION

For the past four centuries, cyclic variations in solar activity have been characterized by smoothed sunspot numbers, which were introduced and classified by Waldmeier (1961) and were selected as the first proxy for solar activity. These numbers show quasi-regular maxima and minima of solar activity changing approximately every 11 years and reflecting the changing magnetic activity of the Sun (Hathaway et al. 2002; Hathaway & Rightmire 2011). Nowadays these sunspot numbers are measured by most solar observatories then averaged and smoothed over all the measurements for each month to produce the smoothed average sunspot numbers published by the National Oceanic and Atmospheric Administration (NOAA; see, as an example, the sunspot activity in Figure 1 in Solanki & Krivova 2011).

The Sun has surprised researchers with its much lower activity in the current cycle 24 compared with that in the previous three cycles 21–23, particularly with regard to its very long minimum period between cycles 23 and 24 (more than two years in 2008–2010) in which there was a lack of any activity at all. This minimum solar activity was evident not only in the lack of sunspots but also in solar magnetic field variations (de Toma et al. 2010a, 2010b), modulation of cosmic rays (McDonald et al. 2010), and in interplanetary coronal mass ejections (Barnard et al. 2011). This prolonged minimum in cycle 24 was all the more surprising because the previous five cycles had been extremely active and so sunspot-productive that they were designated as a Grand Maximum (Solanki et al. 2004; Usoskin 2008; Usoskin et al. 2008; Solanki & Krivova 2011). In cycle 24, the Grand Maximum was followed by much lower solar activity, allowing some authors to suggest that the Sun is on its way toward a Maunder Minimum of activity (Lockwood et al. 2011). This reduced appearance of sunspots in the current cycle 24 was not anticipated by many researchers before the cycle began (see for example Pesnell 2008, and references therein) although after 2003, some researchers predicted a weaker cycle 24 (see for example Svalgaard et al. 2005; Choudhuri et al. 2007).

The smoothed sunspot number had already reached 66.9 (in 2012 February) due to the strong peak in late 2011, so the official maximum will be at least this high (http://www.ngdc.noaa.gov/stp/IONO/sunspot.html). The smoothed sunspot number has been rising again toward a second peak over the last four months and is approaching the level of the first peak (the smoothed sunspot number was 65.6 in July of 2013). The current predicted and observed sizes make this cycle 24 the smallest sunspot cycle since cycle 14, which had a maximum of 64.2 in February of 1906. Using direct polar field measurements available for four solar cycles, Svalgaard et al. (2005) predicted that the approaching solar cycle 24 (2011 maximum) would have a peak monthly smoothed sunspot number of 75 ± 8, making it potentially the smallest cycle in the last 100 yr while Choudhuri et al. (2007) was the only model-related prediction based on the measured polar magnetic fields, which anticipated reduced activity of about 35% in cycle 24.

Prediction of a solar cycle through sunspot numbers has been used for decades as a way of testing our knowledge of the mechanisms of solar dynamo, including the processes providing production, transport, and disintegration of the solar

magnetic field. Most commonly predicted is the sunspot number R_z derived directly from sunspot observations. A number of techniques are used to predict the amplitude of a cycle during the time near and before sunspot minimum. Relationships have been found between the size of the next cycle maximum and the length of the previous cycle, the level of activity at sunspot minimum, and the size of the previous cycle.

However, according to Pesnell (2008), a summary of the predictions for the solar activity in cycle 24 made by more than 30 authors well before it started revealed that all these predictions anticipated a much stronger cycle 24 with a maximum sunspot number well above 100, approaching 185 (Thompson 1993) or 165 (Dikpati et al. 2006) in some predictions, with most authors giving 130–140 (Hathaway & Wilson 2004; Kim et al. 2006; Maris & Oncica 2006). These prediction methods included a number of disturbed days (Thompson 1993), linear regression analysis (Pesnell 2008), neural network forecast (Maris & Oncica 2006), a modified flux-transport dynamo model calibrated with historical sunspot data from middle-to-equator latitudes (Dikpati et al. 2006) or from the polar magnetic field data (Choudhuri et al. 2007), and singular spectral analysis (Loskutov et al. 2001).

This systematic deviation in the predicted solar activity of sunspot numbers from those actually measured in cycle 24 discussed above signals very loudly a significant discrepancy between the processes used in the prediction compared to those defining the solar activity cycle through the action of the solar dynamo. In recent years, a good correlation was found between the polar magnetic field in the solar minimum and the sunspot numbers in the next solar cycle (Kitchatinov & Olemskoy 2011; Muñoz-Jaramillo et al. 2013). The idea behind this close correlation is hidden in the high diffusivity Babcock–Leighton dynamo model, which was proposed by Choudhuri et al. (2007). However, the Babcock–Leighton-type flux transport dynamo model (Karak & Nandy 2012) is shown to produce a reliable prediction for no more than one solar cycle because of the short memory of the dynamo. This conclusion was also supported by Muñoz-Jaramillo et al. (2013) from the correlation of the polar field derived from the observed polar faculae data with the sunspot number.

Independently of a method of prediction, the question remains as to why the action of the solar dynamo, which is associated with both the poloidal magnetic field of the Sun and the toroidal field of sunspots, is tested and predicted using only the characteristics of sunspots. With such an approach, the magnetic field of sunspots formed during the dynamo process and delivered from the bottom of the convective zone to the solar surface is assumed to be linked with sunspots numbers R_z, which in fact, can be different due to the sunspot's magnetic field (associated with the toroidal magnetic field), which is jointly defined by a sunspot's area and its magnetic field strength. This may be the cause of some disagreement between the predicted and observed sunspot activity of the Sun in cycle 24.

However, a number of researchers have already concluded that a different proxy for solar activity is needed, and this proxy is more frequently associated with the solar background magnetic field (SBMF; Hoeksema 1984; Ball et al. 2012; Zharkova et al. 2012; Benevolenskaya 2004, 2013, and references therein). Some researchers consider polar magnetic fields to be a good proxy (Choudhuri et al. 2007; Muñoz-Jaramillo et al. 2013; Benevolenskaya 2004, 2013), while others consider the entire solar magnetic field on the solar disk to be a proxy for the generation of solar irradiance (Ball et al. 2012) or as the main proxy defining the whole picture of the solar activity as observed both in time and in latitudes (Zharkova et al. 2012).

The first relationship between sunspot numbers and the magnetic field of the Sun was derived by exploring the magnetic fields of sunspots (sunspot magnetic fields, SMFs) which were found to be in anti-correlation with the SBMF within an 11 year period (Stix 1976; Zharkov et al. 2008), indicating the main variations in the dipole dynamo waves associated with these fields. Later, a smaller correlation for a period of approximately 2.5 years was established between the SMF and the SBMF (Zharkov et al. 2008), pointing to smaller scale fluctuations of the solar dynamo waves within 2.5 years, in addition to the 11 year period.

In our recent paper (Zharkova et al. 2012), the SBMF and the SMF were analyzed by using principal and independent component analysis that uncovered the two principal temporal magnetic waves originating in the northern and southern hemispheres, both of which traveled over a solar cycle duration to the northern hemisphere in odd cycles 21 and 23 and to the southern hemisphere in even cycle 22. Variations of auto-correlation coefficients in the latitudinal SBMF PCs were also uncovered in different cycles, allowing us to assume a presence of either dipole or quadrupole magnetic sources required for generation of the poloidal field with a given latitudinal profile. In addition, some interrelations between the PCs (and thus, magnetic waves) generated by the SBMF and the SMF in time and latitude are also derived.

The new main issue discovered with this PC approach was the occurrence of pairs of dynamo waves of opposite polarity traveling off-phase with an increasing phase shift, having different amplitudes, and a number of equator crossings in the opposite hemispheres for different cycles (Zharkova et al. 2012). The shapes of the waves allowed the authors to assume a presence not only of dipole but also of quadruple magnetic sources causing these waves and revealed that the wave amplitudes were consistently reduced (by up to 50%) from cycle 21 to cycle 23. Furthermore, the authors showed that the principal components (PCs) of the (toroidal) magnetic field in sunspots follow rather closely the residuals of the temporal PCs in the SBMF (poloidal field) for all three cycles 21–23, pointing out that the sunspot production mechanism can be considered as a *derivative* of the mechanism generating the poloidal magnetic field.

The variations in time and in latitudes of the waves in the SBMF discovered with PC analysis allowed authors to search for the first interpretation of waves derived with a modified two-layer Parker's dynamo model with meridional circulation (Popova et al. 2013). For the first time, the authors were able to simulate latitudinal dynamo waves of the poloidal magnetic field in both hemispheres, fitting them to the derived independent components using three parameters: an amplitude ratio in the hemispheres, a number of zeros or equator crossings, and a phase shift between the components. These simulations detected an interesting tendency in the generation of this poloidal field showing steady increases from cycle 21 to cycle 23 in (a) the dynamo number, (b) the number of equator crossings (zeros), and (c) the phase shifts between the pair of waves.

This critical progress in understanding the links between the visible appearance of the solar activity and the solar dynamo mechanisms used in the model inspired us to explore the derived PCs of the SBMF for prediction of the solar activity by using the most advanced software *Eureqa*, developed on Hamiltonian principles (Schmidt & Lipson 2009). In this paper, we show

that the classic proxy for solar activity, the average sunspot numbers, is strongly modulated by variations in the SBMF PCs, allowing us to suggest *SBMF PCs as a new proxy for solar activity*. Furthermore, by using the *Eureqa* technique based on a symbolic regression, we attempt to uncover the underlying mathematical law governing the variations in the magnetic field of the Sun which might shed more light on the physical mechanisms of magnetic wave generation from the solar dynamo. These invariants are used to extract the key parameters of the PCs of SBMF waves, which are, in turn, used for prediction of the overall level of solar activity for solar cycles 24–26.

The motivation and method used to derive the SBMF wave parameters are described in Section 2; a comparison of the SBMF and SMF PC variations, the prediction results, and the suggestion of a new proxy for solar activity are discussed in Section 3; and conclusions are drawn in Section 4.

2. DISTILLING DYNAMO WAVES FROM THE SBMF PRINCIPAL COMPONENTS

The main challenge in determining a natural law in some observational series is to find a relationship that is a genuine function of the system's state while avoiding the (infinitely many) trivial or meaningless relations that are nothing more than curve fits. Many published invariant quantities have turned out to be coincidental.

In order to have a reasonable degree of confidence in the discovered relation, one ideally needs to infer some invariant property of the system such as the Lagrangian or Hamiltonian (Bongard & Lipson 2007), similar to that developed in the *Eureqa* package (Schmidt & Lipson 2009), which uses symbolic regression to uncover fundamental relationships in data. One systematic way to accomplish this is to restrict our search to systems that can predict differential relationships between two or more variables.

One such relationship that is easy to find from both the equation of the proposed relation and the numerical data is the partial derivative between the pairs of variables. This is the approach we have taken in our quest to uncover the underlying physical law behind the temporal solar background magnetic waves traveling in the northern and southern hemispheres as derived from PC analysis.

2.1. Method of Distilling the Parameters of Complex Waves

We can estimate the partial derivative between any pair of variables from the ratio of their numerical derivatives over time:

$$\frac{\Delta x}{\Delta y} \approx \frac{dx}{dt} \Big/ \frac{dy}{dt}. \quad (1)$$

We can do the same for our candidate law equation, say $f(x,y)$, using the basic calculus:

$$\frac{\Delta x}{\Delta y} \approx \frac{df}{dy} \Big/ \frac{df}{dx}. \quad (2)$$

Hence, now we have two estimates of the partial derivative, one from the numerical data and one from the proposed relationship equation. To measure how well the relation predicts the data, one needs to calculate the mean-log-error ϵ of the difference over the data set:

$$\epsilon \approx \frac{1}{N} \sum_{1}^{N} \cdot \log\left(1 + \left|\left(\frac{\Delta x_i}{\Delta y_i} - \frac{dx_i}{dy_i}\right)\right|\right). \quad (3)$$

This general idea can be extended to higher dimensional symbolic relationships and, in particular, to handling the problem where one variable may be dependent on another as applicable to SBMF and SMF (Zharkova et al. 2012). For example, when taking the partial derivative of $f(x, y, z)$ one cannot, in general, assume independence of all variables. Thus, one needs to perform a symbolic derivative for each possible dependent pairing.

Hence, we can have an approximate derivative in a form either:

$$\frac{\partial}{\partial x}(x^2 + y^2 + z^2) \approx 2x + 2y\frac{\partial y}{\partial x}, \quad (4)$$

or

$$\frac{\partial}{\partial x}(x^2 + y^2 + z^2) \approx 2x + 2z\frac{\partial z}{\partial x}. \quad (5)$$

For a general case, one can choose either equation shown above and compare the fits. For full details of the regression methods applied refer to Schmidt & Lipson (2009).

2.2. Derived SBMF Functionalities

Using the above approach, we took the two time series for the SBMF waves (derived as PCs) plotted in Figure 1 (upper plot) for the 385 Carrington rotations covering the calendar years 1977–2006 (which we call "historical data") and formed their underlying invariants with the relevant parameters derived. Then two main PCs were fitted by *Eureqa* with functional equations for each, from which we calculated the mathematical equations of the temporal dependence of the two PCs written in the general form for component 1 (blue line) as:

$$f(t) = \sum_{k=1}^{N} A_k cos(\omega_{k,1}t + \phi_{k,1}) cos(B_k cos(\omega_{k,2}t + \phi_{k,2})), \quad (6)$$

and for component 2 (red line) as:

$$f(t) = \sum_{k=1}^{N} C_k cos(\omega_{k,3}t + \phi_{k,3}) cos(D_k cos(\omega_{k,4}t + \phi_{k,4})). \quad (7)$$

The product of the two cosine functions ($cos * cos$) accounts for the amplitude modulation of the PC waves over time, while the nested function ($cos(cos)$) represents a frequency modulation term, allowing the waves to change their frequency and phase with time. It was found that $N = 5$ terms allows one to capture the functions describing the waves with an accuracy of better than 98% (see the comparison of the PCs ((dashed lines) and the *Eureqa*-derived curves in Figure 2 (upper plot) and the discussion in Section 3.1).

From these two PCs a summary curve is calculated by adding the amplitudes of the PCs with the appropriate sign. The resulting curve represents the summary activity in the SBMF as plotted in Figures 1 and 2 (bottom plots).

2.3. Analysis of the SBMF Oscillations

The key point is that we do not simply do a curve fitting to experimental data. Instead, with the proposed *Eureqa*'s approach, we are uncovering some genuine underlying mathematical expressions of the oscillations detected from the SMBF with PCA. Having obtained the equations for the actual underlying physical law of the magnetic (dynamo) waves for the SBMF attributed to the poloidal field of the Sun (Popova et al. 2013), one is able to use these equations to make predictions in time, both

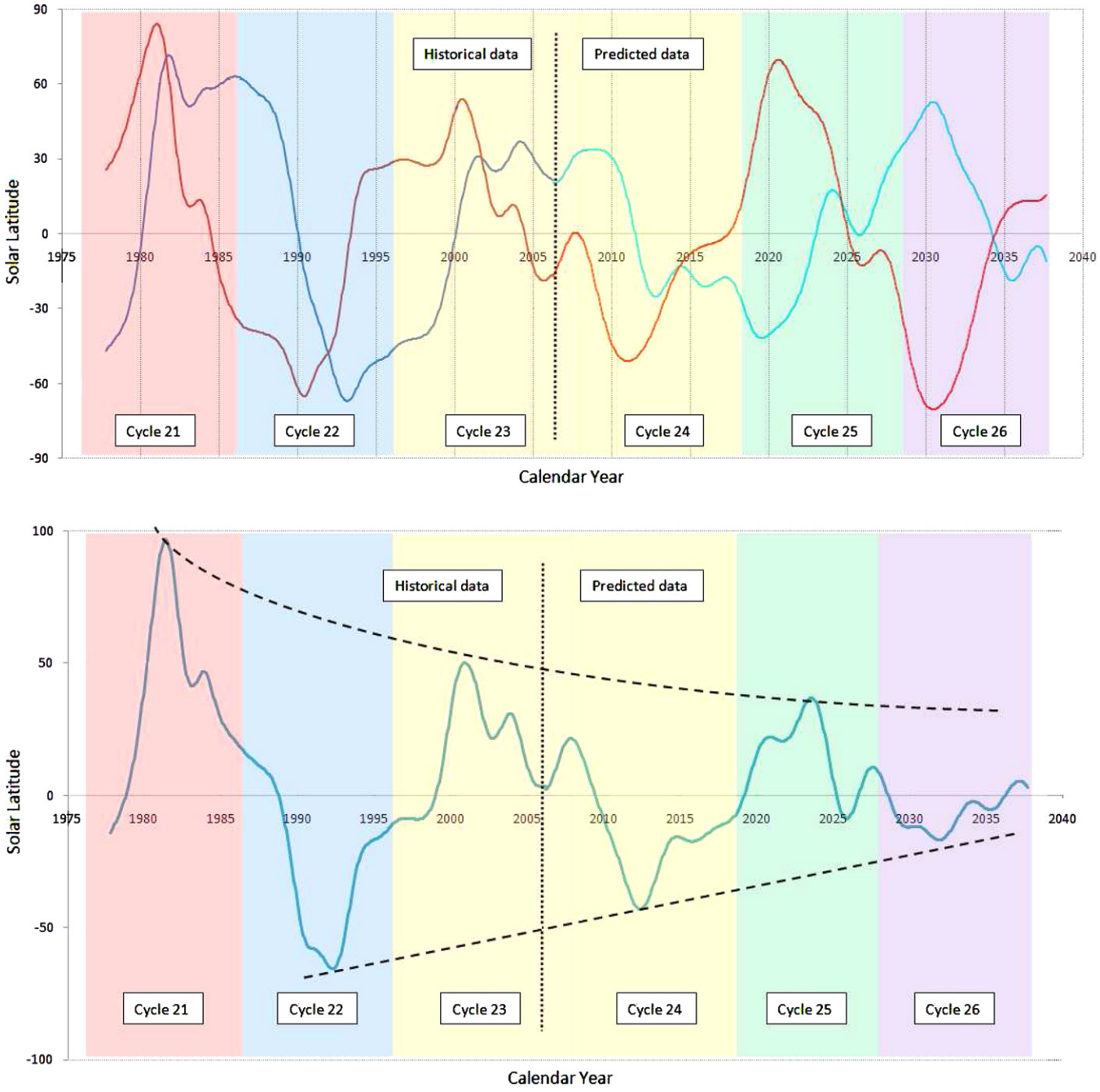

Figure 1. Top plot: the two principal components (PCs) of SBMF (blue and red curves) obtained for cycles 21–23 (historic data, taken from Zharkova et al. 2012) and predicted for cycles 24–26 with the *Eureqa*-derived functionality. Bottom plot: the summary component of the two PCs (solid curve) and the decaying component (dashed curves) for the "historical" data (cycles 21–23) and predicted data (cycles 24–26). The cycle lengths (about 11 yr) are marked with different colors.

(A color version of this figure is available in the online journal.)

forward and backward, from the current epoch and to use them for incorporation into the solar dynamo models.

As shown in the top plot in Figure 1, both of the PCs (blue and red curves) derived from the historical data (full-disk Wilcox Solar Observatory (WSO) magnetograms) in cycles 21–23 show a few clear trends (Zharkova et al. 2012): (1) at the start of data in cycle 21, the oscillations marked by the red curve start in the northern hemisphere while those marked by blue start in the southern hemisphere, (2) both oscillations approach their maxima in the northern hemisphere for odd cycles 21 and 23 or in the southern one for even cycle 22, (3) the maxima of both oscillations overlap in the northern hemisphere for odd cycles 21 and 23 and in the southern hemisphere for even cycle 22, making these hemispheres more active in the given cycle than the opposite ones, and (4) the magnitudes of the maxima for both curves steadily decrease by approximately 30%–40% from cycle 21 to cycle 23.

In order to bring the detected trends in the SBMF closer to the currently used sunspot index, we calculated the summary component of the two PCs (the bottom plot in Figure 1) where we also plotted with a dashed line the curve shown in the area marked as "historic data," a clear decay of the summary component from cycles 21 to 23. The decay is intrinsic to the mechanisms (assumed to be the poloidal magnetic

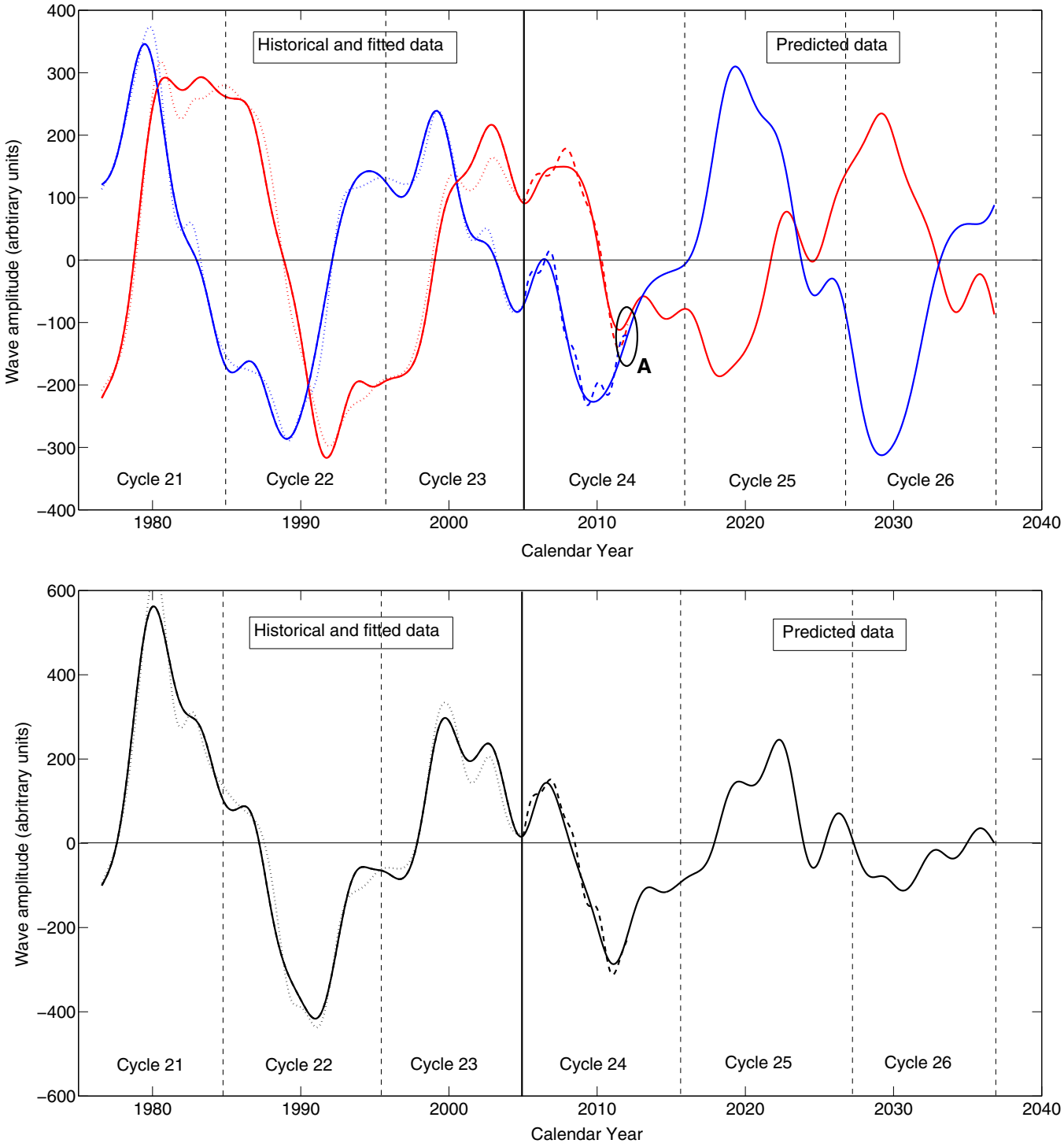

Figure 2. Top plot: the accuracy of the fit with distilled laws from *Eureqa* (solid curves) to the two principal components (PCs) of SBMF (dotted curves) from Figure 1 for cycles 21–23 and their further expansion to cycles 24–26. Bottom plot: the fit of the *Eureqa*-distilled law (the solid curve) to the summary component in cycles 21–23 (dotted curve) and its expansion to cycles 24–26. Dashed curves in both plots show the predicted principal components (top plot) and the summary curve (bottom plot) compared to the real PCs derived from the SBMF in the cycle 24 with an accuracy better than 98%. A letter "A" denotes summer 2014.

(A color version of this figure is available in the online journal.)

field produced by the solar dynamo) responsible for generating the two main waves detected as the two PCs. This decay indicates a decrease in the SBMF from cycles 21 to 23 that was already spotted for the similar data from other observatories, reported by Lockwood et al. (2011) and Solanki & Krivova (2011).

3. PREDICTION OF THE SOLAR ACTIVITY

3.1. Predicted Solar Background Magnetic Field Oscillations

3.1.1. Probing Accuracy and Robustness of Prediction

As explained in Section 2.2, in the current approach we use the historic WSO data marked up to the end of the year 2006 for

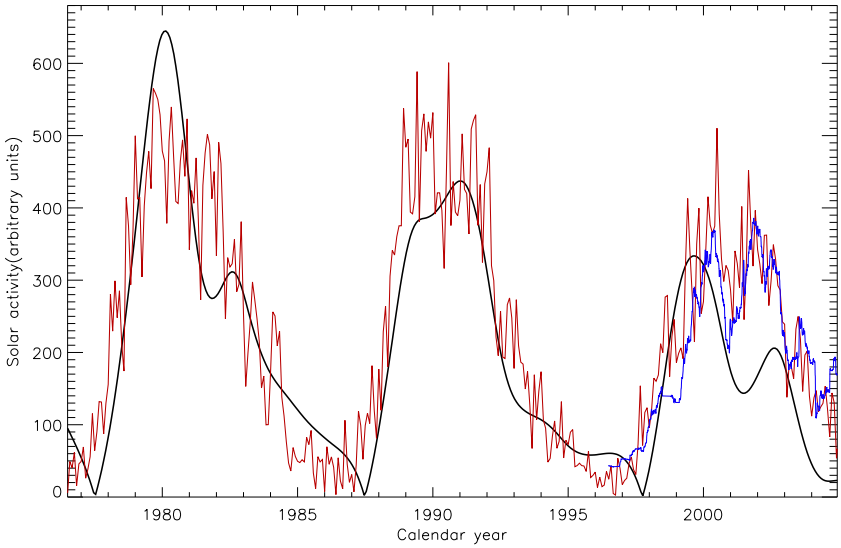

Figure 3. Comparison of the NOAA average sunspot numbers in cycles 21–23 (the purple curve) and the *SOHO*/MDI sunspot magnetic field averaged with 12 months running filter (blue curve) taken from Zharkov et al. (2008) with the modulus summary component (the black curve) derived from the summary SBMF component from Figure 2 (bottom plot).

(A color version of this figure is available in the online journal.)

deriving the functionalities in the PCs of SBMF. The accuracy of the *Eureqa*-derived functionality in Equations (6) and (7) describing the SBMF PCs can thus be checked by a comparison of these *Eureqa*-derived curves with the PCs obtained from SBMF in the WSO data from the end of 2006 (when the training set ended) to summer 2014.

This comparison is plotted in Figure 2 showing a very close (up to 98%) fit to the observational PCs in the period defined for cycle 24, similar to the accuracy of the training set in cycles 21–23. This close fit of the predicted PCs to those derived from the SBMF data in cycle 24 (from 2006 to the calendar year) proves sufficient robustness of the method of prediction described in Section 2.2.

3.1.2. Analysis of SBMF Prediction for Cycles 25–26

Hence, the oscillations of the SBMF will continue to decrease in the next two cycles with a decrease in the amplitude of the summary component for cycle 26 by a factor of four compared to the PC in cycle 21 or by factor of two for cycle 23. Furthermore, the two PCs in cycles 25 and 26 are found to have a large phase shift of about half of the period (10 yr) having opposite signs of the PCs in the periods of the expected solar activity maxima when these waves are expected to interfere with each other in the same hemisphere and to create visible solar activity on its surface in the form of magnetic flux tubes seen as sunspots.

In other words, the PC waves detected in SBMF are predicted to travel with increasing phase shifts approaching nearly an antiphase in the next two cycles when the red wave is only present in the northern (cycle 25) and southern (cycle 26) hemispheres while the blue wave travels in the southern (cycle 25) and the northern (cycle 26) hemispheres. This can result in the absence of many of the visible signs of SBMF variations listed at the start of the Section 2.3 (Zharkova et al. 2012) and thus, in the lack of solar activity in general in the classic sense of sunspot appearances. In order to understand the effect of SBMF variations on solar activity, we investigate the links between these two features (SBMF PCs and sunspot index) in the historic data in Section 3.2 and establish whether they have some significance in predicting solar activity.

3.2. Summary of the SBMF Component as a Solar Activity Proxy

As discussed in the Introduction, most prediction models for solar activity use average sunspot numbers in various attempts to predict their variation in future solar cycles. The lack of strongly positive fits of predicted solar activity (in sunspot numbers) with real solar activity measured later, after the prediction has been made, indicates consistent disagreement between the variables defining solar activity as modeled in dynamo models (poloidal and toroidal magnetic fields) and those measured (average sunspot numbers).

In the current study, we suggest using the two PCs of the SBMFs for cycles 21–23 derived from the principal component analysis as plotted in Figure 1 and their summary component calculated as a sum of the derived PCs as proxies. In Figure 3 this summary component is converted into the modulus summary curve (e.g., making all negative values of the PCs positive; the black curve) and plotted versus averaged sunspot numbers (red curve) taken from NOAA Web site and the sunspot magnetic fluxes in cycle 23 (the blue curve) measured with *Solar and Heliospheric Observatory* (*SOHO*)/MDI (Zharkov et al. 2008) and averaged with 18 months running filter.

One can note a remarkable resemblance between the modulus summary curve and the curves describing the averaged smoothed sunspot numbers or the averaged sunspot magnetic flux in cycles 21–23 with a small exception for the descending phase of cycle 23. Both curves show the double maxima of the solar activity first reported by Gnevyshev (Gnevyshev & Ol' 1987) and clearly observed in cycles 21–23, although the SMF variations in the descending phase of cycle 23 seem to trail the sunspot numbers, indicating that the magnetic field magnitude within sunspots is increasing toward the minimum of the solar activity. The latter tendency indicates an increase at the descending phase of magnetic field strength (or the toroidal magnetic field) within sunspots through their stronger twists and shears,

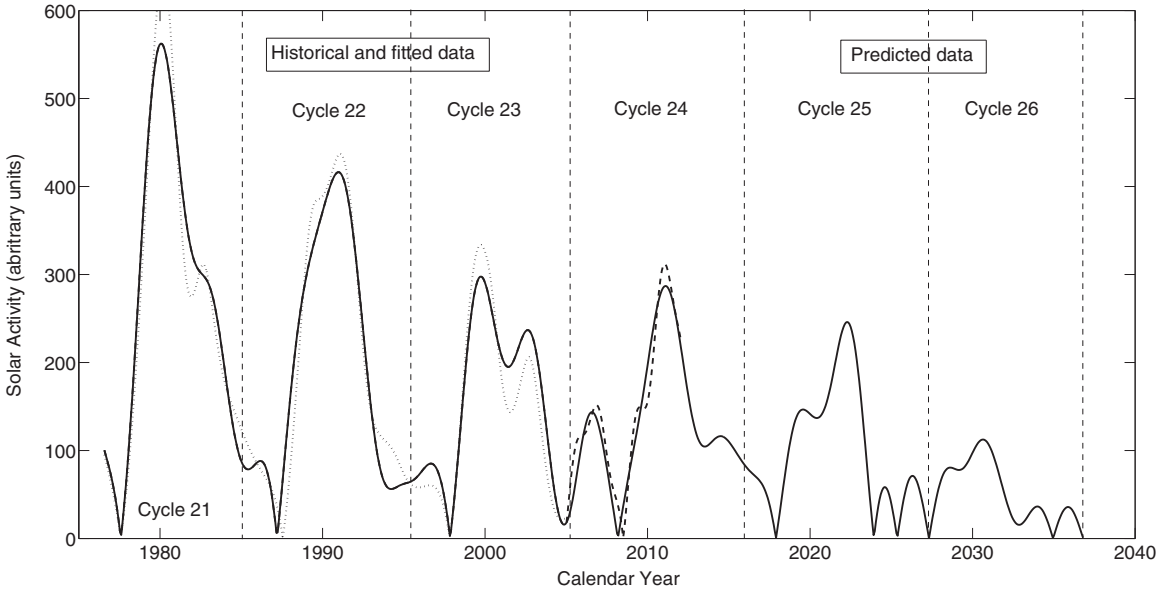

Figure 4. Modulus summary principal component (solid curve) calculated from Equations (6) and (7) for cycles 21–23 and predicted for cycles 24–26, the modulus summary PC derived from SBMF in cycles 21–23 (dotted curve) and in cycle 24 (dashed curve).

which will result in an increase of the line-of-sight magnetic field component that needs to be tested with future modeling.

The prediction of this modulus summary curve for cycles 25 and 26 presented in Figure 4 allows us to see a noticeable decrease in the predicted average sunspot numbers in cycle 25 to ≈80% of that in cycle 24 and ≈40% in cycle 26 which is linked to a reduction of the amplitudes and an increase in the phases of the PCs of SBMF discussed above. Hence, on the one hand, this modulus summary curve is found to be a good proxy for the traditional solar activity contained in the averaged sunspot numbers. On the other hand, however, this summary curve is a derivative of the PCs of SBMF with clear mathematical functionalities simultaneously representing the real physical process—poloidal field dynamo waves—generated by the solar dynamo (Popova et al. 2013).

Therefore, the modulus summary curve proves that the PCs of SBMF can be considered very good proxies for the traditional solar activity understood by many observers whereas for the prediction of the solar activity in cycles 24–26 and for modeling the solar dynamo processes, in general, it is much more beneficial to use the two PCs derived from PCs with *Eureqa*, as they distil a number of the real modes of dynamo waves derived from SBMF with principal component analysis.

Based on the similarity of the modulus summary and sunspot curves, one can conclude that the solar activity in cycles 24–26 will be systematically decreasing because of the separation into the opposite hemispheres and, thus, a lack of interaction between the two dynamo waves of the poloidal magnetic field. This separation can result in the absence of magnetic flux tubes appearing on the solar surface as sunspots possibly leading to a lack of any sunspot activity on the solar surface, similar to that recorded during the Maunder Minimum in the medieval period.

4. CONCLUSIONS

In the current study, to predict the solar activity, we explore the PCs derived from the SBMF measured with the WSO in cycles 21–23 by using the most advanced *Eureqa* approach developed on Hamiltonian principles (Schmidt & Lipson 2009). We show that the classic proxy for solar activity, averaged sunspot numbers, is strongly modulated by variations in the SBMF PCs, allowing us to use the *SBMF PCs as new proxies* for the overall solar activity.

Furthermore, by using the *Eureqa* technique based on a symbolic regression, we managed to uncover the underlying mathematical laws governing the fundamental processes of magnetic wave generation in the Sun's background magnetic field. These invariants are used to extract the key parameters of the PCs of SBMF waves, which, in turn, are used to predict the overall level of solar activity for solar cycles 24–26.

We can conclude with a sufficient degree of confidence that the solar activity in cycles 24–26 will be systematically decreasing because of the increasing phase shift between the two magnetic waves of the poloidal field leading to their full separation into opposite hemispheres in cycles 25 and 26. This separation is expected to result in the lack of their subsequent interaction in any of the hemispheres, possibly leading to a lack of noticeable sunspot activity on the solar surface lasting for a decade or two, similar to those recorded in the medieval period.

Using the modulus summary curves derived from the principal components of SBMF, we predict a noticeable decrease of the average sunspot numbers in cycle 25 to ≈80% of that in cycle 24 and a decrease in cycle 26 to ≈40% which are linked to a reduction of the amplitudes and an increase of the phase between the PCs of SBMF separating these waves into the opposite hemispheres. We propose using the PCs derived from SBMF as a new proxy for the solar activity which can be linked more closely to dynamo model simulations.

Further investigation is required to establish more precise links between the dynamo waves generated by both poloidal and toroidal magnetic fields as simulated in the dynamo models and the waves in the solar background (SBMF) and sunspot (SMF) magnetic fields derived with the PC and symbolic regression analysis presented in the current study which will be the scope of a forthcoming paper.

The authors thank the WSO staff and directorate for providing the synoptic maps of the solar background magnetic field for usage by a general public. We also express our deep gratitude to

the respected referee for very constructive and useful comments from which the paper has strongly benefited.

REFERENCES

Ball, W. T., Unruh, Y. C., Krivova, N. A., et al. 2012, A&A, 541, A27
Barnard, L., Lockwood, M., Hapgood, M. A., et al. 2011, GeoRL, 38, 16103
Benevolenskaya, E. E. 2004, A&A, 428, 5
Benevolenskaya, E. E. 2013, Ge&Ae, 53, 891
Bongard, J., & Lipson, H. 2007, PNAS, 104, 9943
Choudhuri, A. R., Chatterjee, P., & Jiang, J. 2007, PhRvL, 98, 131103
de Toma, G., Gibson, S., Emery, B., & Kozyra, J. 2010a, in AIP Conf. Proc. 1216, Twelfth International Solar Wind Conference, ed. M. Maksimovic et al. (Melville, NY: AIP), 667
de Toma, G., Gibson, S. E., Emery, B. A., & Arge, C. N. 2010b, in ASP Conf. Ser. 428, SOHO-23: Understanding a Peculiar Solar Minimum, ed. S. R. Cranmer, J. T. Hoeksema, & J. L. Kohl (San Francisco, CA: ASP), 217
Dikpati, M., de Toma, G., & Gilman, P. A. 2006, GeoRL, 33, 5102
Gnevyshev, M. N., & Ol', A. I. 1987, BSolD, 1987, 90
Hathaway, D. H., & Rightmire, L. 2011, ApJ, 729, 80
Hathaway, D. H., & Wilson, R. M. 2004, SoPh, 224, 5
Hathaway, D. H., Wilson, R. M., & Reichmann, E. J. 2002, SoPh, 211, 357
Hoeksema, J. T. 1984, PhD thesisStanford Univ., CA
Karak, B. B., & Nandy, D. 2012, ApJL, 761, L13
Kim, M. Y., Wilson, J. W., & Cucinotta, F. A. 2006, AdSpR, 37, 1741
Kitchatinov, L. L., & Olemskoy, S. V. 2011, AstL, 37, 656
Lockwood, M., Owens, M. J., Barnard, L., Davis, C. J., & Steinhilber, F. 2011, GeoRL, 38, 22105
Loskutov, A. Y., Istomin, I. A., Kotlyarov, O. L., & Kuzanyan, K. M. 2001, AstL, 27, 745
Maris, G., & Oncica, A. 2006, SunGe, 1, 8
McDonald, F. B., Webber, W. R., & Reames, D. V. 2010, GeoRL, 37, 18101
Muñoz-Jaramillo, A., Dasi-Espuig, M., Balmaceda, L. A., & DeLuca, E. E. 2013, ApJL, 767, L25
Pesnell, W. D. 2008, SoPh, 252, 209
Popova, E., Zharkova, V., & Zharkov, S. 2013, AnGeo, 31, 2023
Schmidt, M., & Lipson, H. 2009, Sci, 324, 81
Solanki, S. K., & Krivova, N. A. 2011, Sci, 334, 916
Solanki, S. K., Usoskin, I. G., Kromer, B., Schüssler, M., & Beer, J. 2004, Natur, 431, 1084
Stix, M. 1976, A&A, 47, 243
Svalgaard, L., Cliver, E. W., & Kamide, Y. 2005, GeoRL, 32, 1104
Thompson, R. J. 1993, SoPh, 148, 383
Usoskin, I., Solanki, S., & Kovaltsov, G. 2008, in COSPAR Meeting, Vol. 37, 37th COSPAR Scientific Assembly, 3264
Usoskin, I. G. 2008, LRSP, 5, 3
Waldmeier, M. 1961, The Sunspot-activity in the Years 1610–1960 (Zurich: Schulthess)
Zharkov, S., Gavryuseva, E., & Zharkova, V. 2008, SoPh, 248, 339
Zharkova, V. V., Shepherd, S. J., & Zharkov, S. I. 2012, MNRAS, 424, 2943